

Structural, Magnetic, and Electronic Properties of the NiO Monolayer Epitaxially Grown on the (001) Ag Surface: An *ab Initio* Density Functional Study

S. Casassa,* A. M. Ferrari, M. Busso, and C. Pisani

Unità INFN di Torino, Sezione F, and Dipartimento di Chimica IFM, Università di Torino,
via Giuria 5, I-10125 Torino, Italy

Received: July 4, 2002; In Final Form: October 9, 2002

A periodic slab model consisting of five layers of Ag covered on both sides by NiO monolayers has been adopted to simulate the properties of ultrathin layers of nickel oxide epitaxially grown on silver (001). Different *ab initio* approaches have been tested including unrestricted Hartree–Fock and a variety of hybrid-exchange density functional Hamiltonians. The hybrid Becke3–Perdew–Wang functional (containing a 20% fraction of Hartree–Fock exchange) has been selected because of its satisfactory performance in describing the experimentally known properties of the two bulk systems, silver and nickel oxide. All calculations have been performed with the CRYSTAL program. In the most stable configuration (O ions directly above Ag atoms, Ni above the hollow sites), the oxide surface is corrugated (0.1 Å) and a small reduction of the work function of the metal is observed (~ 0.1 eV). The AFM1 antiferromagnetic structure (alternating rows of nickel ions with opposite spin along the [11] direction) is the most stable one both in the isolated and in the supported monolayer. The Ni–Ni superexchange constant (J_2) is appreciably increased (30%) by the presence of the Ag substrate. In conclusion, the presence of the metallic substrate has been found to influence the structural, electronic, and magnetic properties of the overlayer but only to a limited extent.

1. Introduction

The present paper deals with the study of the interface between silver and an epitaxial overlayer of nickel oxide. In the last years, the preparation and characterization of these two-dimensional materials have become a topic of great interest, both experimentally and theoretically. In catalysis, for example, it has been suggested that the structural and electronic properties of the substrate can significantly influence the reactivity of the oxide overlayers, leading to potentially new catalytic mechanisms. In particular, some recent studies^{1,2} have proposed that oxide–metal interfaces may have peculiar chemical and physical properties because of image potential screening of charge transfers and interfacial hybridizational effects.

The model system for most of these studies has been the MgO/Ag interface. Despite a great deal of work, there are still controversial issues concerning this system between experimental and theoretical analysis. XPS spectra^{1,3} support the hypothesis of strong interaction between the two subunits, characterized by a wide hybridization between the two band structures and an appreciable enhancement of the oxide reactivity. On the contrary, an *ab initio* quantum-mechanical investigation⁴ proposes a rather different picture: the silver substrate has some influence on the structural and electronic properties of the oxide but only at the interface. The increase in the reactivity has been suggested to be due to the presence of structural and point defects.

The case of NiO/Ag might be qualitatively different from MgO/Ag despite the structural similarity of the two systems (both oxides exhibit fcc structure, and their (001) nonpolar face grows epitaxially on the Ag (001) surface). The main gap in NiO is much smaller (~ 4 eV) than is the case of MgO (~ 8 eV), and opens in the minority set of d bands: hybridization with metal states might be then much easier. Moreover, if

magnetic order is preserved in the oxide after the interface formation, a nonnegligible spin polarization could be induced in the surface Ag atoms. From an experimental point of view, NiO/Ag is a more difficult system to deal with, and only recently considerable successes have been achieved in its realization and characterization.^{5,2} The lattice mismatch of 2% between the two bulk structures is small enough to prevent the formation of catastrophic structural defects,⁵ and “perfect” thin films, on the order of 5 monolayers and even less, have been deposited and fully characterized.² Nevertheless, some authors claim that the epitaxial nature of the film is not so firmly established and that the reactivity could be determined to some extent by lattice defects.⁶

Modeling of the NiO/Ag interface could provide complementary information with respect to the experimental investigations and could clarify some aspects of the latter. This is true, for instance, as concerns XPS spectra, the analysis of which is difficult because of the importance of initial state and final state effects. Theoretical investigations also present some difficulties. First, it is not trivial to select a quantum-mechanical *ab initio* approach capable of describing at the same level of accuracy both a metal and a magnetic insulator; furthermore, a periodic model is necessary to take into account both short and long-range Coulomb effects, which play a fundamental role in the characteristics of the electronic structure of the interface.

In this work, we present a quantum-mechanical *ab initio* study of the fundamental state of NiO/Ag(001) based on the use of a periodic model and of a hybrid-exchange B3PW Hamiltonian as implemented in the public code CRYSTAL.⁷ The paper is organized as follows.

In section 2, the theoretical framework and the computational parameters are presented. This study is at the confluence of two long-lasting projects undertaken in our group regarding the characterization of metal/oxide interfaces and the investigation

of the magnetic properties of bulk materials. For this reason, a certain amount of know-how has been used in the selection of basis set, geometries, computational parameters, and Hamiltonians. As concerns the last point, we briefly analyze the reasons for adopting the B3PW Hamiltonian. The next two sections are devoted to the description of the noninteracting systems. Section 3 provides new data on the Ag slab, modeled as a five-layer film and described by means of the hybrid-exchange Hamiltonian; these are compared with those previously published for a six-layer Ag slab, studied with a different density functional theory (DFT) Hamiltonian.⁴ Both geometry and electronic structure are reproduced at a good level of accuracy.

An investigation of the nonsupported NiO monolayer with reference to the corresponding bulk structure is presented in section 4. The choice of a suitable Hamiltonian capable of reproducing both the magnetic and electronic properties of a solid is still an open problem.⁸ Nevertheless, recent studies on NiO bulk^{9,10} have demonstrated that a DFT hybrid approach yields a reasonable description of structural parameters, magnetic constants, and magnitude of the band gap. To check whether the monolayer can be treated at this level, we have considered a set of different Hamiltonians, ranging from Hartree–Fock (HF) to a pure DFT approach. The effect of the percentage of “exact exchange” on the calculated properties of the two main magnetically ordered structures of the monolayer, namely, ferromagnetic (FM) and antiferromagnetic (AFM1, alternating¹¹ rows of nickel atoms with opposite spin), has been studied with reference to the corresponding ones of the bulk. The results for the monolayer are compared to those of a preceding very accurate HF study by Noguera and Mackrodt.¹¹ The model adopted for the interface (a five-layer Ag film sandwiched between two NiO monolayers) is presented and analyzed in section 5. The results are discussed with reference to those for the two isolated subsystems to better appreciate the modifications produced by the interaction. As was the case with MgO/Ag,⁴ no qualitative new features appear associated with the interaction; in particular, the electronic and magnetic structure of the adsorbed film is not changed in any essential way with respect to the unsupported film. On the other hand, the energy distribution of virtual nickel states in a vicinity of the Fermi level is appreciably modified. These results are discussed with reference to recent experimental studies.¹

2. Computational Details

The calculations were performed by means of a beta version of the CRYSTAL computer code, which solves the Schrödinger equation for periodic systems both in a HF¹² and in a DFT¹³ framework. CRYSTAL adopts a set of localized Gaussian-type functions (GTF) centered in the atomic nuclei and with the angular features of standard atomic orbitals; each crystalline orbital is in turn described by a linear combination of such atomic orbitals.

The effective-core pseudopotential technique¹⁴ was used for silver and nickel atoms to reduce the number of electrons involved and the complexity of the calculations. The number of electrons explicitly considered is 19 per Ag atom and 16 per Ni ion (corresponding to the electronic configurations 4s²4p⁶4d¹⁰5s¹ and 3s²3p⁶3d⁸, respectively). The variational basis set for the outer electrons of silver, comprising 4, 4, and 2 GTFs of type s, p, and d, respectively, with a contraction scheme 3111/2211/41, is that optimized by Sgroi et al.⁴ and coincides with one previously used¹⁵ except that the outermost p GTF has been split in two (with exponents 0.32 and 0.15). Nickel has been described with the [HAYWLC]3sp/2d basis set optimized for

bulk nickel oxide by Freyria Fava¹⁶ with the contraction scheme 311/41. The all-electron oxygen basis set, used in previous work on bulk NiO,¹⁷ contains 1s and 3sp contracted GTFs in the scheme 8/411. The quality of these basis sets has proved adequate for the description of the noninteracting systems. The cutoff parameters ITOL 1–5 of CRYSTAL¹² for Coulomb and exchange integrals evaluation have been set to very strict values (7,7,7,7,14). Integration in reciprocal space has been carried out using a Monkhorst grid¹⁸ yielding 45 and 81 *k* points in the irreducible part of the first Brillouin zone for the FM and AFM1 structures, respectively; note that in the latter case symmetry is reduced from square (*P4/mmm* space group) to rectangular (*Pmmm*).

A much more delicate issue has been the choice and calibration of a suitable Hamiltonian, apt to provide a satisfactory description of the properties of such different materials as a metal and a magnetic insulator. Our previous study⁴ has shown that a DFT approach based on the generalized gradient approximation as proposed by Perdew and Wang,¹⁹ to be indicated as PWGGA, performs satisfactorily for the evaluation of the structural and electronic properties not only of MgO but also of silver.⁴ For the latter system, the HF technique has confirmed its well-known inadequacy to describe metals due to its neglect of correlation of electronic motions in the conduction band. On the other hand, a number of recent studies^{9,10,17} have demonstrated that DFT functionals meet with serious difficulties in the description of magnetic insulators. In these systems, the presence of highly localized unpaired electrons requires a very accurate description of nonlocal exchange interactions, which is not properly achieved either with local or gradient-corrected Kohn–Sham Hamiltonians. As a result, their use gives too low spin densities and too narrow band gaps; this contrasts with HF descriptions, which present the opposite defects. Hybrid-exchange Hamiltonians as proposed by Becke,²⁰ which have met extraordinary success in the field of molecular quantum studies, appear a natural option to explore for solving this kind of problem. Their use has been considered therefore by different authors and shown to provide a reliable description of the insulating character and magnetic properties of bulk NiO.^{9,10} We have here systematically explored the influence of the fraction of exact exchange on the calculated properties of NiO monolayer, as was done in the accurate study by Moreira et al.¹⁰ for bulk NiO; our aim was that of selecting a quantum-mechanical technique capable of providing reasonable results for both the silver surface and the oxide thin film. Reference has been made to the following semiempirical formula for the exchange–correlation energy:²⁰

$$E_{XC}^{\text{hybrid,PW}} = E_{XC}^{\text{LSDA}} + a_0(E_X^{\text{HF}} - E_X^{\text{LSDA}}) + a_X\Delta E_X^{\text{B88}} + a_C\Delta E_C^{\text{PW}} \quad (1)$$

Here, LSDA is the local spin density approximation composed of the Dirac–Slater exchange²¹ and the Vosko, Wilk, and Nusair²² correlation functional; HF represents the *exact* part of the exchange energy; B88²³ is Becke’s gradient correction for exchange; PW is the gradient correction for correlation of the PWGGA Hamiltonian. In fact, this last term is the only difference with respect to the original Becke proposal and to the class of Hamiltonians explored by Moreira et al. who used instead the LYP correlation functional.²⁴ The empirical coefficients a_0 , a_X , and a_C have been given the values 0.2, 0.72, and 0.81 by Becke on the basis of a best-fit study of the ground-state energy of a number of small molecules;²⁰ the resulting Hamiltonian is known with the name B3LYP. Surprisingly

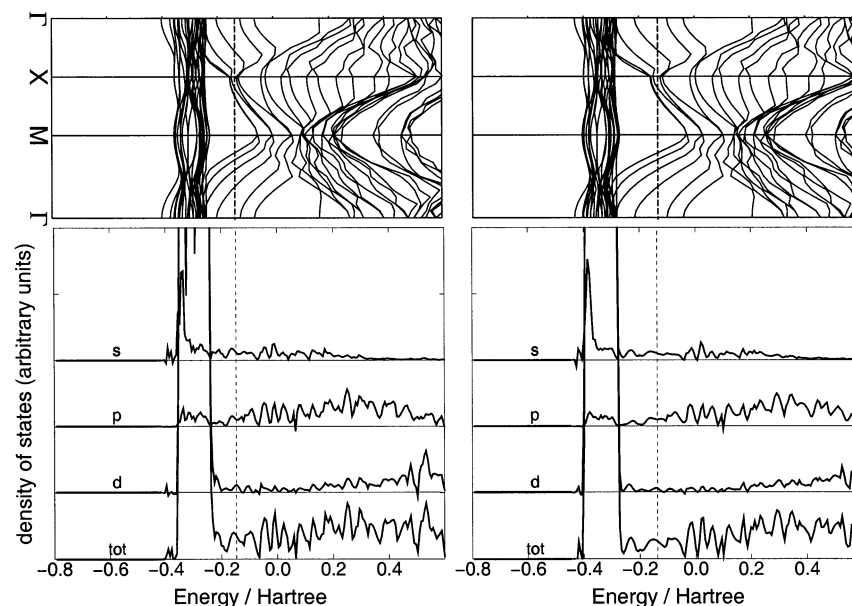


Figure 1. Band structure (top panels) and density of states (DOS) (bottom panels) of the Ag five-layer slab evaluated by means of the PWGGA (left) and B3PW (right) Hamiltonian. The energy scale is the same in the plots above and those below (1 hartree = 27.21 eV). In all panels, the position of the Fermi level is indicated by the vertical dashed line. The DOSs are projected in the subspace of the d, p, and s atomic orbitals of silver, as indicated.

enough, this approach and the related parametrization have proved to perform quite well also for ionic compounds,²⁵ a class of systems very different from those selected for adjusting the B3LYP Hamiltonian. In the present study, only the value of the a_0 parameter was systematically changed from 0 (pure DFT) to 0.5, and the results were compared with those obtained with the unrestricted HF (UHF) approximation; in the case where $a_0 = 0.2$, the Hamiltonian will be referred to as B3PW.

As in the study of Moreira,¹⁰ the magnetic coupling occurring in the NiO monolayer has been investigated by means of the Ising spin Hamiltonian:

$$H^I = -J_1 \sum_{i,j} S_z^i S_z^j - J_2 \sum_{k,l} S_z^k S_z^l \quad (2)$$

where S_z^i stands for the z component of total spin on the magnetic center, and \sum' and \sum'' are extended to first and second neighbors, respectively. The use of such a simplified model permits us to relate the energy of the magnetic phases FM (all Ni spins aligned), AFM1 (alternating [11] rows of nickel atoms with opposite spin), and AFM2 (as before but in the [01] direction) to the magnetic coupling constants J_1 and J_2 . The energy difference per formula unit between these phases is expressed by the following equations:

$$E(\text{AFM2}) - E(\text{FM}) = 4J_1 \quad (3)$$

$$E(\text{AFM1}) - E(\text{FM}) = 2J_1 + 4J_2 \quad (4)$$

3. The Silver Film

A film composed of five atomic layers of Ag parallel to the (001) surface has been used as a model of the metal surface. This thickness is adequate to avoid undesired interaction between the two coadsorbed NiO monolayers and realizes a reasonable compromise between convergence of surface properties and computational cost. The previous study on silver^{4,26} has shown that a good description of the bulk can be achieved using the PWGGA Hamiltonian: the calculated cohesive energy, 2.97 eV, and the (001) surface formation energy, 0.0191 eV,

practically coincide with the respective experimental values,²⁷ and the optimized lattice parameter (4.14 Å) is only 1% larger than experiment²⁸ (4.09 Å). The distribution of one-electron levels and the shape of the Fermi surface are also satisfactory. Similar results have been reported by Doll and Harrison.²⁹ Because however the use of a hybrid exchange Hamiltonian seems necessary for a qualitatively correct description of the oxide (see next section), we have verified whether the use of B3PW is appropriate also with the metallic support.

For the bulk, we get very similar results: the optimized lattice parameter of 4.15 Å corresponds to a cohesive energy of 2.62 eV. In the characterization of the (001) surface, the B3PW Hamiltonian accurately reproduces the electronic structure obtained by means of the PWGGA functional. A comparison between the two band structures, reported in the top panels of Figure 1, shows the strong similarities between the two approaches. The projected density of states (PDOS), bottom panels of Figure 1, clearly indicate that in both cases states at the Fermi level are mainly associated with s and p orbitals, with a minor d contribution. For a slab, the calculated Fermi level, E_F , can be directly related to the opposite of the experimental work function. The latter has been measured by means of XPS³⁰ to be 4.64 eV, while the PWGGA and B3PW values of E_F are -3.7 and -3.6 eV, respectively. Another bulk experimental observable is the distance between the Fermi level and the top of the d band, the measured value³¹ of which is 3.8 eV, intermediate between the PWGGA (2.7 eV) and the B3PW (4.2 eV) estimates. The B3PW surface formation energy is 0.921 J m⁻² in fair agreement with the experimental value²⁸ (1.24–1.32 J m⁻²) and with the already cited studies.^{4,29} As concerns possible relaxation effects of the silver surface, these have been found almost negligible in our previous study, in agreement with experimental LEED results,³² according to which the contraction of the surface is only 1–2% of the interplanar distance. In the following, surface relaxation is disregarded, and the optimized PWGGA lattice parameter (4.14 Å) will be used both for the Ag substrate and for the oxide overlayers.

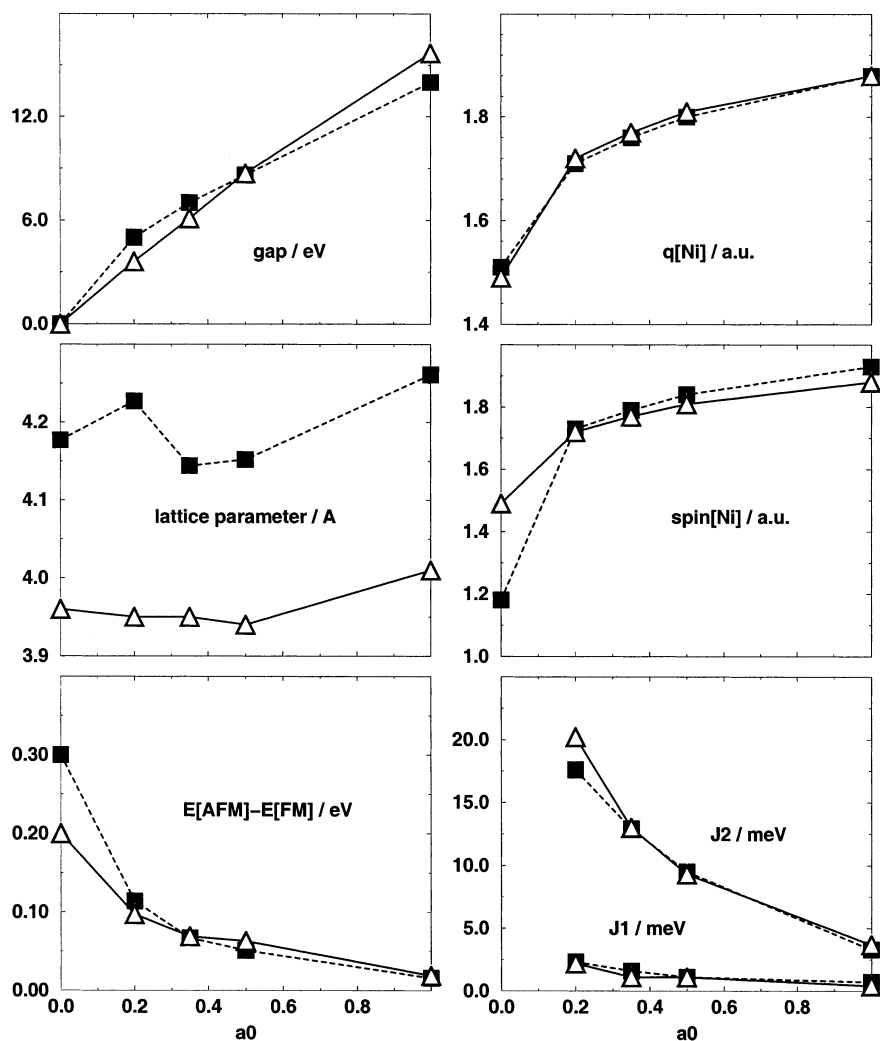


Figure 2. Effect of the a_0 parameter in eq 1 on some properties of bulk NiO (■) and of the isolated monolayer (△). The data for $a_0 = 1$ correspond in fact to UHF calculations. From top to bottom and from left to right, gap is the width of the main gap (experimental value for the bulk³³ is 4.0 eV); lattice parameter is the distance between second neighbor oxygen ions (experimental value for the bulk³⁴ is 4.1705 Å); $E[\text{FM}]$ and $E[\text{AFM}]$ are the energies of the ferromagnetic and of the most stable antiferromagnetic configuration (AFM2 for the bulk, AFM1 for the monolayer); $q[\text{Ni}]$ and $\text{spin}[\text{Ni}]$ designate the net charge and spin population on nickel atoms evaluated according to a Mulliken population analysis; J_1 and J_2 are the magnetic coupling constants (see eq 3) (experimental values^{35,36} are $J_1 < 1.4$ meV and $-19.8 < J_2 < -17.0$ meV).

4. NiO Monolayer versus Bulk Properties

As anticipated in sections 1 and 2, we have systematically explored the effect of the a_0 parameter in eq 1 on the electronic and magnetic properties of bulk NiO and of the isolated (001) NiO monolayer. The a_0 values 0, 0.2 (B3PW), 0.35, and 0.5 have been considered, plus the UHF case, which is made formally to correspond in the following to the value $a_0 = 1$. The aim was twofold, first, to verify whether this choice provided results of comparable quality to those obtained with the hybrid B3LYP Hamiltonian^{9,10} and, second, to check whether new features appeared in the two-dimensional with respect to the three-dimensional structure and how critically these could depend on the adopted Hamiltonian. The essential results of this study are reported in Figure 2; others are provided along with the following comments. (a) All properties change rather regularly with a_0 , but the change can be critically important, in particular, as concerns the passage from an insulating to a conducting character for both structures when a_0 becomes zero. In general, no qualitative differences are observed between bulk and monolayer. (b) With increasing a_0 , the ionic character, the spin localization and the width of the main gap increase; when $a_0 = 0.2$, the value of the latter is 3.6 and 5.0 eV for the

monolayer and the bulk in their stable antiferromagnetic configuration, respectively, to be compared with the experimental bulk value³³ of 4.0 eV. (c) Instead, the change of the equilibrium lattice parameter with a_0 is not monotonic but always close for the bulk to 4.1705 Å, the experimental value.³⁴ At the B3PW level, the isolated monolayer experiences a contraction of about 6% with respect to the optimized bulk lattice parameter. Using the same lattice parameter as for the Ag slab, 4.14 Å, corresponds to an energy cost of about 0.2 eV per NiO unit. This cost is almost as large as the energy of interaction between the monolayer and the substrate (see section 5); therefore, stacking defaults could easily appear at very low coverage, while the mismatch should be reduced when thicker overlayers are considered. (d) In agreement with the detailed UHF study by Noguera and Mackrodt,¹¹ we have found that, independently of the spin order and of the value of a_0 , the most stable Ni(d⁸) atomic configuration is $[(xy)^2(xz)^2(yz)^2(z^2)^1(x^2 - y^2)^1]$ as in the bulk; this is due to the strong in-plane Coulomb interactions and contrasts the fact that the reduced dimensionality induces a change in the ligand-field ordering (the z^2 orbital should be the most stable one in this respect). The resulting asymmetry of the electron charge distribution around the two

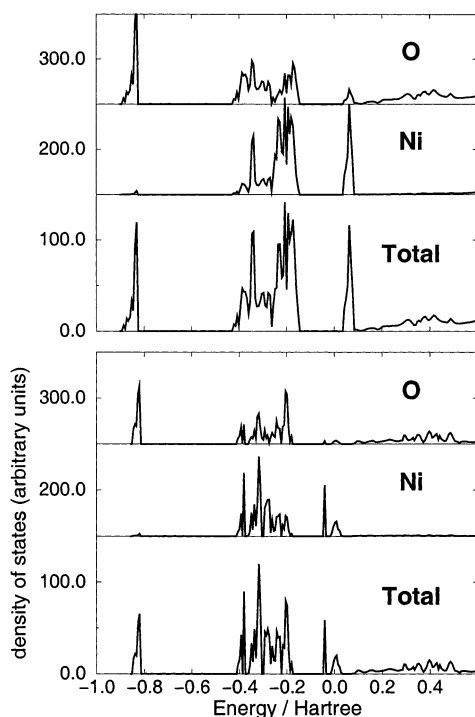


Figure 3. Total and projected densities of states of the two stable antiferromagnetic structures of NiO bulk (top) and of the NiO (001) monolayer (bottom). Both calculations are performed at the B3PW level.

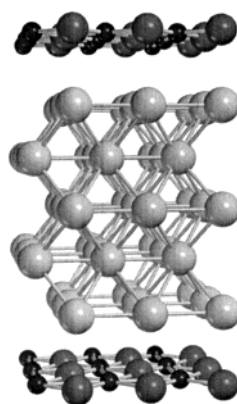


Figure 4. Model for the NiO/Ag interface. The stable “B” configuration is represented here with oxygens (large spheres) above surface silver atoms and nickel atoms above hollow surface sites.

ions (both exhibiting large quadrupole moments) explains the strong contraction of the monolayer lattice parameter with respect to the bulk, which has no counterpart in the MgO case. (e) The stability order of the different magnetic structures is also independent of a_0 : for the monolayer, AFM1 is the most stable one, followed by FM and AFM2, as already established in the UHF case.¹¹ However, the energy differences decrease rapidly with a_0 . (f) The absolute values of the J_1 and J_2 parameters, see eqs 3 and 4, also decrease with increasing a_0 ; in particular, the bulk B3PW ($a_0 = 0.2$) estimate of J_2 , -17.6 meV, is close to the experimental value,^{35,36} -19.0 ± 1 meV, while it is only -3.3 meV in the UHF case. Again, the bulk and monolayer values of the two coupling constants follow a very similar pattern. This confirms the results of a recent theoretical study by de Graaf et al.,³⁷ which adopts sophisticated cluster techniques, disproving the hypothesis that the superexchange interaction might become much stronger when going from bulk to a (001) surface of late transition metal oxides.³⁸

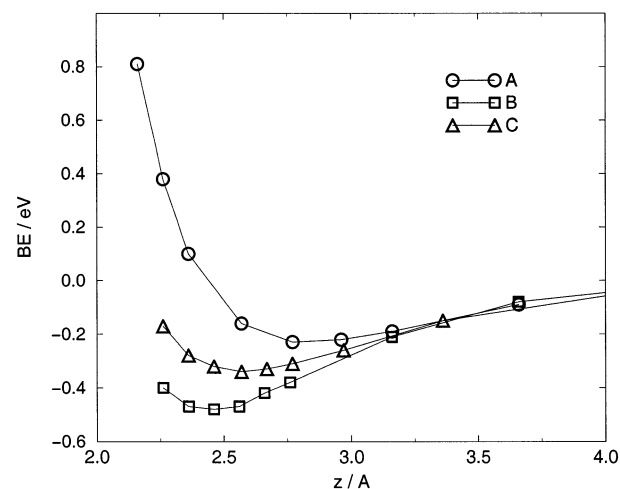


Figure 5. Interaction energy (BE) per NiO unit between the five-layer Ag slab and the NiO monolayer as a function of the distance z for the three configurations A, B, and C. The data are referred to B3PW calculations, FM ordering in the overlayer, and a flat (NORUMP) geometry. No BSSE corrections are included. The three equilibrium distances of 2.77, 2.44, and 2.57 Å, correspond to BE values of -0.23 , -0.48 , and -0.34 eV, respectively.

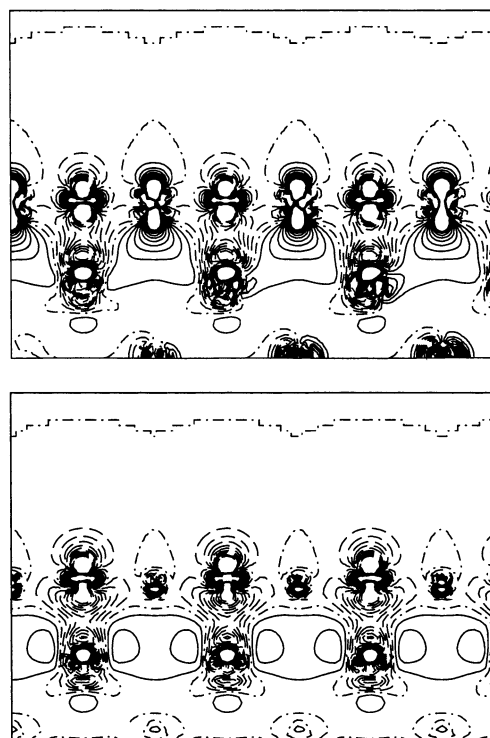


Figure 6. Difference density maps for NiO/Ag and MgO/Ag. The plots show the difference between the electron density for the compound system and the superposition of the electron densities of the two corresponding subunits with the same internal geometry. Left panel presents NiO/Ag in AFM1 RUMP configuration. Right panel presents MgO/Ag in RUMP configuration. The sections are in a vertical plane through the [01] direction, exhibiting the sequence of ...M-O-M-O... atoms, the oxygens lying above the silver surface atoms. The spacing between consecutive density isolines is 0.001 au; continuous, dot-dash, and dashed lines refer to positive, zero, and negative density difference, respectively.

In summary, the B3PW Hamiltonian appears to provide a satisfactory description of bulk NiO in all respects. We have assumed the same to be true for the two-dimensional structure because no essential differences are encountered between the

TABLE 1: Geometric, Energetic, and Electronic Properties of the Interfaces Calculated with the B3PW Hamiltonian^a

	NiO/Ag FM		NiO/Ag AFM1		MgO/Ag	
	NORUMP	RUMP	NORUMP	RUMP	NORUMP	RUMP
BE (eV)	0.23	0.25	0.23	0.26	0.13	0.22
d_M (Å)	2.44	2.36	2.45	2.35	2.57	2.44
d_O (Å)	2.44	2.44	2.45	2.45	2.57	2.57
E_f (eV)	-2.56	-3.35	-2.52	-3.47	.30	-2.01
q_M (Δ^*)	1.68 (-0.06)	1.69 (-0.05)	1.67 (-0.05)	1.68 (-0.04)	1.89 (0.00)	1.89 (0.00)
q_O (Δ^*)	-1.66 (0.08)	-1.63 (0.11)	-1.65 (0.07)	1.60 (0.12)	-1.78 (0.11)	-1.72 (0.18)
q_{Ag} (Δ^*)	-0.04 (-0.02)	-0.09 (-0.07)	-0.05 (-0.03)	-0.10 (-0.08)	-0.11 (-0.09)	-0.18 (-0.16)
μ_{Ni} (Δ^*)	1.70 (-0.11)	1.71 (-0.10)	± 1.68 (∓ 0.09)	± 1.69 (∓ 0.08)		
μ_O (Δ^*)	0.15 (-0.04)	0.15 (-0.04)	0.0	0.0		
μ_{Ag}	-0.05	-0.05	0.0	0.0		

^a The MgO data have been recalculated with the present B3PW Hamiltonian and by considering a five-layer silver slab as a support. The columns "NORUMP" and "RUMP" are referred to the flat and corrugated equilibrium geometry of the overlayer, respectively. BE are the binding energies per NiO (or MgO) unit corrected for the BSSE (which amounts to 0.25 and 0.27 eV in the NORUMP and RUMP cases, respectively). d_M and d_O are the distances of the metal cation (Ni or Mg) and of the oxygen anion from the surface plane of the silver slab. The Fermi level of the isolated five-layer Ag slab is -3.59 eV. Electronic net charges (q) and spin populations (μ) are evaluated according to a Mulliken population analysis and are expressed in au; those labeled Ag refer to surface silver atoms. The Δ^* data in parentheses indicate the change of the respective quantity in the compound system with respect to the noninteracting subunits.

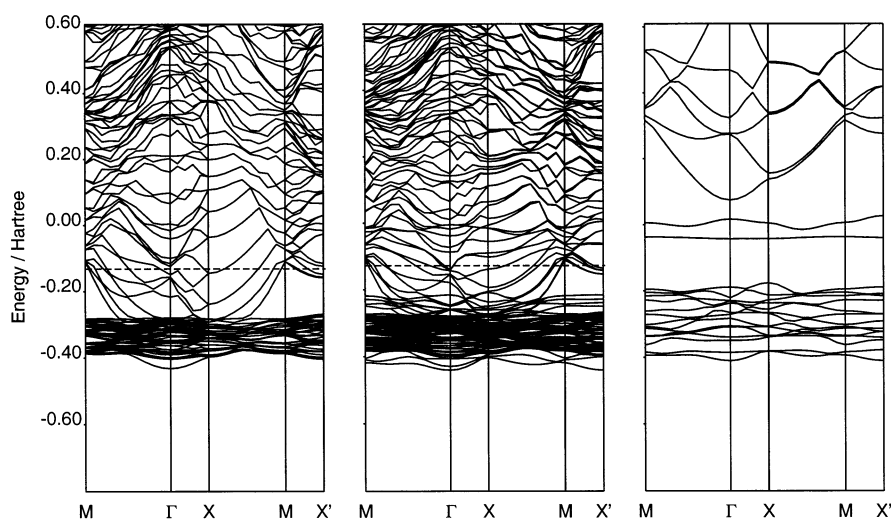


Figure 7. Band structure of the Ag five-layer slab (left), of the NiO/Ag compound system with rumpling allowed (center), and of the NiO monolayer (right). In the last two cases, the magnetic structure is AFM1; the corresponding reciprocal lattice cell is a rectangle centered in Γ with X and X' at the center of the long and short side, respectively, and M at a vertex. For consistency, the same cell has been adopted for the Ag slab. The dashed line gives the position of the Fermi energy.

two cases. Because this Hamiltonian is also adequate for the silver slab, from now on all results are referred to that choice.

The B3PW total and projected DOSs of the bulk and the monolayer are compared in Figure 3. The appreciable reduction of the main gap in the latter case is seen to be mainly due to a splitting of the unoccupied d bands into two, the lower one associated with z^2 and the other with $x^2 - y^2$ atomic orbitals. Also in the manifold of the occupied d bands, the singly occupied ones, those with z^2 and $x^2 - y^2$ character, split out from the others at the low-energy end. The $O(2p) \rightarrow Ni(3d)$ nature of the main gap is particularly evident for the monolayer, where participation of O p orbitals is dominant at the top of the valence bands.

5. NiO on Ag

The model adopted for the present study is represented in Figure 4. As in the case of MgO,⁴ three high-symmetry geometries have been studied: (A) Ni^{2+} over a surface Ag atom and O^{2-} over a hollow site; (B) the same, but with the two ions interchanged; (C) both ions over a bridge position. The distance between the silver surface and the oxide overlayer was optimized, first considering the NiO film as a rigid entity

(NORUMP) and then allowing the two sublattices to move independently in the z direction (RUMP). Binding energies versus distance between the NiO overlayer and the silver substrate are reported in Figure 5 for the NORUMP, ferromagnetic case. Allowing rumpling of the overlayer or changing its magnetic structure does not change significantly these curves. In the rest of the paper, only the results for the most stable B configuration are presented and discussed.

The main results are collected in Table 1 and compared with those for the MgO monolayer. The basis set superposition error³⁹ (BSSE) has been evaluated by calculating the energy of the isolated systems, Ag slab and NiO monolayer, surrounded by ghost functions in the position of the adsorbed oxide film and of the adsorbing metal, respectively. Binding energies, equilibrium geometries, and charge distributions are seen to be essentially unaffected by the magnetic order because of the dominant electrostatic character of the interaction. We note incidentally that the order of stabilities of the different magnetic structures of the overlayer is the same as in the unsupported film. It is interesting to observe that the equilibrium distance between the overlayer and the silver surface is shorter, the rumpling less important, and the interaction energy higher than

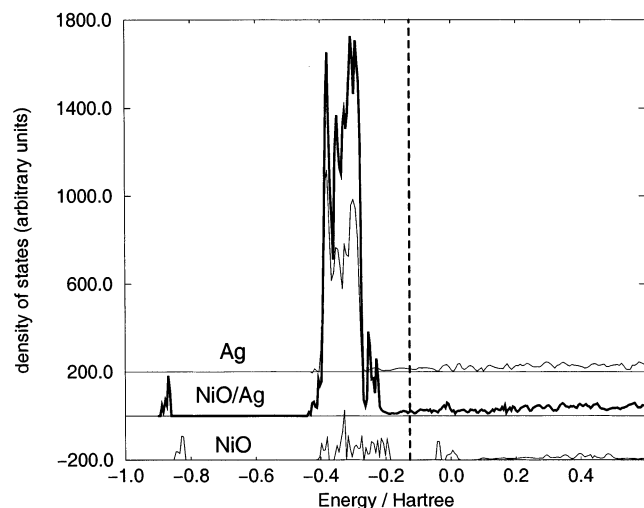


Figure 8. Total density of states of NiO/Ag and of the two noninteracting subunits. The position of the Fermi level for the compound system is indicated by the vertical dashed line.

in the case of MgO. These effects are probably related to the lesser ionicity of the NiO film, which reduces Pauli repulsions between the oxygen anions and the underlying silver atoms, so permitting closer approach between the two subunits. The lesser ionicity also explains why “electron transfer” from oxygens to the silver film is less important in the present case; as a consequence of that, the change in the Fermi energy associated with the double layer of charges at the surface (see our previous study⁴ for a detailed discussion) is much less relevant, 0.12 instead of 1.58 eV. Comparison of the difference density maps reported in Figure 6 better clarifies differences and similarities of the charge redistribution between the two supported oxides: in both cases, some extra electron density appears in the interstices between surface silver atoms, but this effect is more evident with MgO than with NiO. It is also seen that the positive charge on Mg is unaffected by the interaction with silver, while that of Ni decreases, essentially because of partial repopulation of the virtual z^2 orbitals. To state it in a more quantitative way, the decrease of the net Mulliken charges of Ni from 1.73 to 1.68 au is associated with an *increase* of the z^2 electron populations from 1.024 to 1.126 au and a parallel but less important *decrease* of $x^2 - y^2$ from 1.196 to 1.145 au. The repopulation of the minority-spin states explains why spin localization in the NiO film is slightly reduced after interaction with the silver slab. The fact that the B3PW magnetic coupling constants, J_1 and J_2 , are appreciably higher (3.45 and -32.1 meV) than those in the unsupported film (3.45 and -32.1 meV) is also probably to be attributed to the enhanced spin population of the in-plane $x^2 - y^2$ orbitals. Finally note that no appreciable magnetic effects are induced by the overlayer on the silver film: a small spin image is found on surface Ag atoms only in the FM case, probably mediated by the oxygen ions.

Further information about electronic effects occurring at the interface can be gathered from Figures 7, 8, and 9, which compare band structure and DOSs of the compound system NiO/Ag with those of the noninteracting subunits. The three band structures support the idea that the interaction between the two subsystems has the character of a weak physisorption: the bands of the compound system are essentially the superposition of those of the constituent units, even in a vicinity of the Fermi energy, except for a slight, rigid displacement. The total DOSs of Figure 8 confirm this picture; the partial depopulation of oxygens, with an increase of virtual at the expense of occupied projected DOSs, is responsible for the net lowering of the

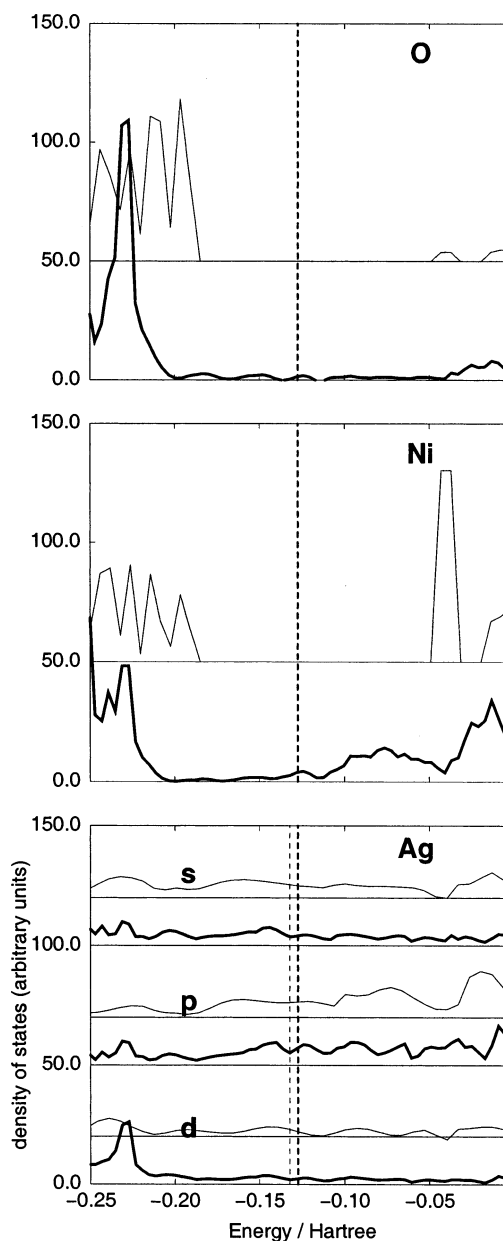


Figure 9. Projected densities of states of NiO/Ag (bold lines) and of the two noninteracting subunits (light lines) in a proximity of E_F . The position of the Fermi level is indicated by the vertical dashed lines: bold for NiO/Ag, nonbold for the silver slab. The projections are effected according to a Mulliken population analysis; in the case of silver, they refer to surface atoms. All densities are referred to the respective zero line; they are strictly comparable because the vertical scale is the same in all plots.

average position of the O s band from -22.7 to -23.8 eV. The PDOSs in a vicinity of the Fermi level (see Figure 9) reveal finer details of the mode of interaction. It is seen that the virtual Ni z^2 states become much less localized and their distribution extends practically down to the Fermi level. The effective nickel oxide gap at the interface is more than halved with respect to the free monolayer value. In fact, there appears to be a nonnegligible contribution of nickel to the conductivity properties of the film. However, the characterization of nickel as a $3d^8$ ion is only marginally affected.

6. Discussion and Conclusions

As concerns structural data, a first confirmation of our results comes from a recent XAFS study⁴⁰ regarding overlayers of NiO

(3–10 layers) on a silver substrate. The measured Ni–Ag distances appear in good agreement with our present findings; however, to verify the effects of the oxide thickness on the geometry of the atoms at the interface, we are performing accurate calculations on a two-layer NiO/Ag system.

The agreement with the experiment is not as satisfactory when considering other physical properties. On the basis of XPS experiments,¹ some authors have hypothesized a drastic change in the electronic structure of the NiO overlayer. They found a spectrum for the supported oxide that is very similar to that of metallic nickel and suggested as a possible explanation that the ground-state electronic configuration of the Ni ions in the supported monolayer is not $3d^8$ as in bulk NiO but rather a mixture of $3d^9$ and $3d^{10}$ as in Ni metal. The occurrence of such a band occupation is ascribed to the possibility for the Ni 3d unoccupied bands of crossing the Ag Fermi energy with a strong hybridization between the Ag 5sp, 4d bands and the NiO states.

The present calculations have shown that the presence of a silver substrate modifies indeed the structural (surface corrugation) and electronic (charge transfer) properties of an epitaxial oxide monolayer. At the same time, the oxide perturbs the substrate by inducing electric polarization of the interface, which causes a small reduction of the work function of the metal. These effects are similar but less important than those in the case of an MgO overlayer. On the whole, the supported film appears to be still characterized as a $Ni^{2+}O^{2-}$ ionic system with Coulomb interactions determining its stability and structure, in contrast with the interpretation of the experiments just recalled. Nevertheless, interesting changes are seen in the distribution of nickel virtual states, which could have relevant consequences in simulated XPS spectra.

It can finally be questioned how suitable the present calculations are for interpreting this kind of experiments. As concerns the computational method adopted, the somewhat empirical exploration of a variety of Hamiltonians has lead us to select a hybrid method that appears adequate to describe the properties of both bulk silver and nickel oxide; we do not see special reasons why the same should not be true as concerns the description of the corresponding two-dimensional structures and their interaction. The second, perhaps more fundamental, objection is that the adopted model (defect-free, infinitely periodic, perfectly epitaxial structures) may not be a faithful representation of the actual systems investigated by experimentalists.

Acknowledgment. The present work is part of the PRA/ISADORA project coordinated by G. Pacchioni and financed by the Istituto Nazionale di Fisica della Materia. Useful discussions with S. Valeri, A. Altieri, G. Pacchioni, and I. P. R. Moreira are gratefully acknowledged.

References and Notes

- (1) Altieri, S.; Tjeng, L. H.; Sawatzky, G. A. *Thin Solid Films* **2001**, *400*, 9.
- (2) Luches, P.; Altieri, S.; Giovanardi, C.; Moia, T. S.; Valeri, S.; Bruno, F.; Floreano, L.; Morgante, A.; Santaniello, A.; Verdini, A.; Gotter, R.; Hibma, T. *Thin Solid Films* **2001**, *400*, 139.
- (3) Altieri, S. Electronic Structure of Oxide Thin Film on Metals. Ph.D. Thesis, University of Groningen, Groningen, Netherlands, 1999.
- (4) Sgroi, M.; Pisani, C.; Busso, M. *Thin Solid Films* **2001**, *400*, 64.
- (5) Wollschläger, J.; Erdös, D.; Goldbach, H.; Höpken, R.; Schröder, K. M. *Thin Solid Films* **2001**, *400*, 1.
- (6) Portalupi, M.; Duò, L.; Isella, G.; Bertacco, R.; Marcon, M.; Ciccacci, F. *Phys. Rev. B* **2001**, *64*, 165402.
- (7) Saunders, V. R.; Dovesi, R.; Roetti, C.; Causà, M.; Harrison, N. M.; Orlando, R.; Zicovich-Wilson, C. M. *Crystal98 User's Manual*; Università di Torino: Torino, Italy, 1998.
- (8) Harrison, N. M.; Saunders, V. R.; Dovesi, R.; Mackrodt, W. C. *Philos. Trans. R. Soc. London, Ser. A* **1998**, *356*, 75.
- (9) Muscat, J.; Wander, A.; Harrison, N. M. *Chem. Phys. Lett.* **2001**, *342*, 397.
- (10) Moreira, I. P. R.; Illas, F.; Martin, R. L. *Phys. Rev. B* **2002**, *65*, 155102.
- (11) Noguera, C.; Mackrodt, W. C. *J. Phys.: Condens. Matter* **2000**, *12*, 2163.
- (12) Pisani, C.; Dovesi, R.; Roetti, C. *Hartree–Fock Ab Initio Treatment of Crystalline Systems*; Lecture Notes in Chemistry, Vol. 48; Springer: Berlin, 1988.
- (13) Towler, M. D.; Zupan, A.; Causà, M. *Comput. Phys. Commun.* **1996**, *98*, 181.
- (14) Hay, P. J.; Wadt, W. R. *J. Chem. Phys.* **1985**, *82*, 270.
- (15) Doll, K.; Pykkö, P.; Stoll, H. *J. Chem. Phys.* **1998**, *109*, 2339. www.chimifm.unito.it/teorica/crystal/Basis_Sets.
- (16) Freyria Fava, F. *Tesi di Laurea*; Università di Torino: Torino, Italy, 1997.
- (17) Mallia, G.; Orlando, R.; Llunell, M.; Dovesi, R. *NATO Science Series III (Computer and System Science)*; IOS Press: Amsterdam, in press.
- (18) Monkhorst, H. J. *Phys. Rev. B* **1969**, *20*, 1504.
- (19) Perdew, J. P. *Electronic Structure of solids*; Akademie Verlag: Berlin, 1991.
- (20) Becke, A. D. *J. Chem. Phys.* **1993**, *98*, 5648.
- (21) Dirac, P. A. M. *Proc. Cambridge Philos. Soc.* **1930**, *26*, 376.
- (22) Vosko, S. H.; Wilk, L.; Nusair, M. *Can. J. Phys.* **1980**, *58*, 1200.
- (23) Becke, A. D. *Phys. Rev. A* **1988**, *38*, 3098.
- (24) Lee, C.; Yang, W.; Parr, R. G. *Phys. Rev. B* **1988**, *37*, 785.
- (25) Baranek, P.; Lichanot, A.; Orlando, R.; Dovesi, R. *Chem. Phys. Lett.* **2001**, *240*, 362.
- (26) Sgroi, M. *Tesi di Laurea*; Università di Torino: Torino, Italy, 2000.
- (27) Gschneider, K. A. *Solid State Phys.* **1964**, *16*, 276.
- (28) Kittel, C. *Introduction to solid state physics*; Wiley: New York, 1975.
- (29) Doll, K.; Harrison, N. M. *Phys. Rev. B* **2001**, *63*, 165410.
- (30) Dwydari, A. W.; Mee, C. H. B. *Phys. Status Solidi* **1975**, *27*, 233.
- (31) Nilsson, P. O.; Sandell, B. *Solid State Commun.* **1970**, *8*, 712.
- (32) Rhodin, T. N.; Ertl, G. *The nature of the surface chemical bond*; North-Holland: Amsterdam, 1979.
- (33) Sawatzky, G. A.; Allen, J. W. *Phys. Rev. Lett.* **1984**, *53*, 2339.
- (34) Bartel, L. C.; Morosin, B. *Phys. Rev. B* **1971**, *3*, 1039.
- (35) Hutchings, M. T.; Samuelsen, E. J. *Phys. Rev. B* **1972**, *6*, 3447.
- (36) Shanker, R.; Singh, R. A. *Phys. Rev. B* **1973**, *7*, 5000.
- (37) De Graaf, C.; Broer, R.; Nieuwpoort, W. C. *Chem. Phys. Lett.* **1997**, *271*, 372.
- (38) Pothuizen, J. J. M.; Cohen, O.; Sawatzky, G. A. *Mater. Res. Soc. Symp. Proc.* **1996**, *401*, 501.
- (39) Boys, S. F.; Bernardi, F. *Mol. Phys.* **1970**, *19*, 553. Davidson, E. R.; Feller, D. *Chem. Rev.* **1986**, *86*, 681.
- (40) Groppo, E.; Lamberti, C. Private communication, July 2002.